Mechanistic and Physiological Implications of the Interplay among Iron-Sulfur Clusters in [FeFe]-Hydrogenases. A QM/MM Perspective

Greco, Claudio; Bruschi, Maurizio; Fantucci, Piercarlo; Ryde, Ulf; De Gioia, Luca

Published in:
Journal of the American Chemical Society

DOI:
10.1021/ja205542k

2011

Mechanistic and physiological implications of the interplay among iron–sulfur clusters in [FeFe]-hydrogenases. A QM/MM perspective.

Claudio Greco[a,b]*, *Maurizio Bruschi*[c], *Piercarlo Fantucci*[a], *Ulf Ryde*[d], *Luca De Gioia*[a,]*

[a] Department of Biotecnology and Bioscience, University of Milan-Bicocca, Piazza della Scienza 2, 20126, Milan (Italy); [b] Department of Chemistry, Humboldt University of Berlin, Brook-Taylor-Str. 2, 12489, Berlin (Germany); [c] Department of Environmental Sciences, University of Milan-Bicocca, Piazza della Scienza 1, 20126, Milan (Italy); [d] Department of Theoretical Chemistry, Lund University, P.O. Box 124, 22100 Lund (Sweden)

RECEIVED DATE (to be automatically inserted after your manuscript is accepted)

Corresponding authors:

Claudio Greco: claudio.greco@unimib.it; tel. +390264483473, fax: +390264482890

Luca De Gioia: luca.degioia@unimib.it; tel. +390264483463, fax: +390264482890

ABSTRACT

Key stereoelectronic properties of *Desulfovibrio desulfuricans* [FeFe]-hydrogenase (DdH) were investigated by quantum mechanical description of its complete inorganic core, which includes a Fe_6S_6 active site (the H-cluster), as well as two ancillary Fe_4S_4 assemblies (the F and F' clusters). The partially oxidized, active-ready form of DdH is able to efficiently bind dihydrogen, thus starting H_2 oxidation catalysis. The calculations allow us to unambiguously assign a mixed Fe(II)Fe(I) state to the catalytic core of the active-ready enzyme and show that H_2 uptake exerts subtle, yet crucial influences on the redox properties of DdH. In fact, H_2 binding can promote electron transfer from the H-cluster to the solvent-exposed F'-cluster, thanks to a 50% decrease of the energy gap between the HOMO (that is localized on the H-cluster) and the LUMO (which is centered on the F'-cluster). Our results also indicate that the binding of the redox partners of DdH in proximity of its F'-cluster can trigger one-electron oxidation of the H_2-bound enzyme, a process that is expected to have an important role in H_2 activation. Our findings are analyzed not only from a mechanistic perspective, but also in consideration of the physiological role of DdH. In fact, this enzyme is known to be able to catalyze both the oxidation and the evolution of H_2, depending on the cellular metabolic requirements. Hints for the design of targeted mutations that could lead to the enhancement of the oxidizing properties of DdH are proposed and discussed.

Introduction

[FeFe]-hydrogenases are iron-containing enzymes that efficiently catalyze the reversible oxidation of H_2. The chemistry of this enzyme class depends on the unique features of an organometallic cofactor, the H-cluster (Figure 1). The latter is composed of two subclusters covalently linked to each other by the sulfur atom of a cysteine residue,[1-4] viz. an Fe_4S_4 subcluster – named $[4Fe{-}4S]_H$ in the following – and an Fe_2S_2 assembly directly involved in substrate binding. The latter subcluster is usually termed $[2Fe]_H$ and it includes biologically unusual ligands, viz. three carbonyls (one of which in a (semi-)bridging position),[2,5] two cyanides, and a dithiolate ligand that, according to recent spectroscopic,[6] biochemical[7] and theoretical[8] investigations, should be a di(thiomethyl)amine (DTMA) residue.

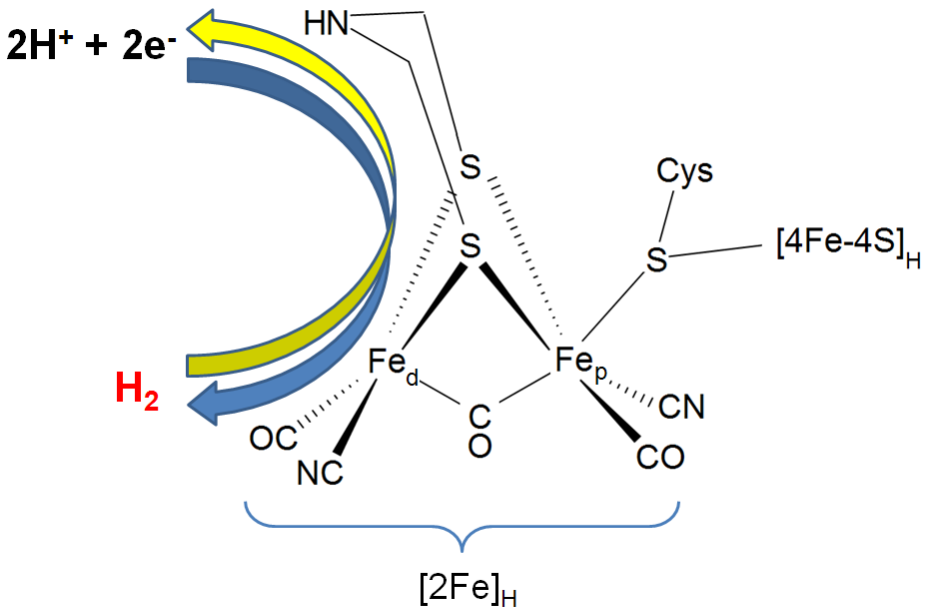

Figure 1. Structural features of the H-cluster: the [FeFe]-hydrogenases active site, directly involved in H_2 evolution and oxidation.

The Mössbauer, electron paramagnetic resonance (EPR), and electron-nuclear double resonance (ENDOR) properties of the [FeFe]-hydrogenases characterized up to now are largely superimposable[12-17] and highlight a complex redox chemistry, owing to the presence of ancillary iron–sulfur clusters that flank the H-cluster in most of the known [FeFe]-hydrogenases. The conservation of the amino acids in the vicinity of the cofactors suggests that the redox properties of the metal clusters are finely tuned to control [FeFe]-hydrogenases function. For example, the reversibility of dihydrogen oxidation catalysis is thought to depend on a tight balance of the redox potential of the catalytic and ancillary clusters.[12] However, only few details are known about the interplay between the H-cluster and the other Fe–S clusters in [FeFe]-hydrogenases.

The [FeFe]-hydrogenases from *Desulfovibrio desulfuricans* (DdH) and *D. vulgaris* Hildenborough (DvH), which share the same amino-acid sequence,[13,18,19] have undergone extensive characterization,[12,17] and the structure of DdH has also been resolved by X-ray spectroscopy.[1] In addition, DdH includes not only the H-cluster, but also two classical ferredoxin-like Fe_4S_4 clusters, which in the following will be referred to as the accessory F and F' clusters (Fig. 2).

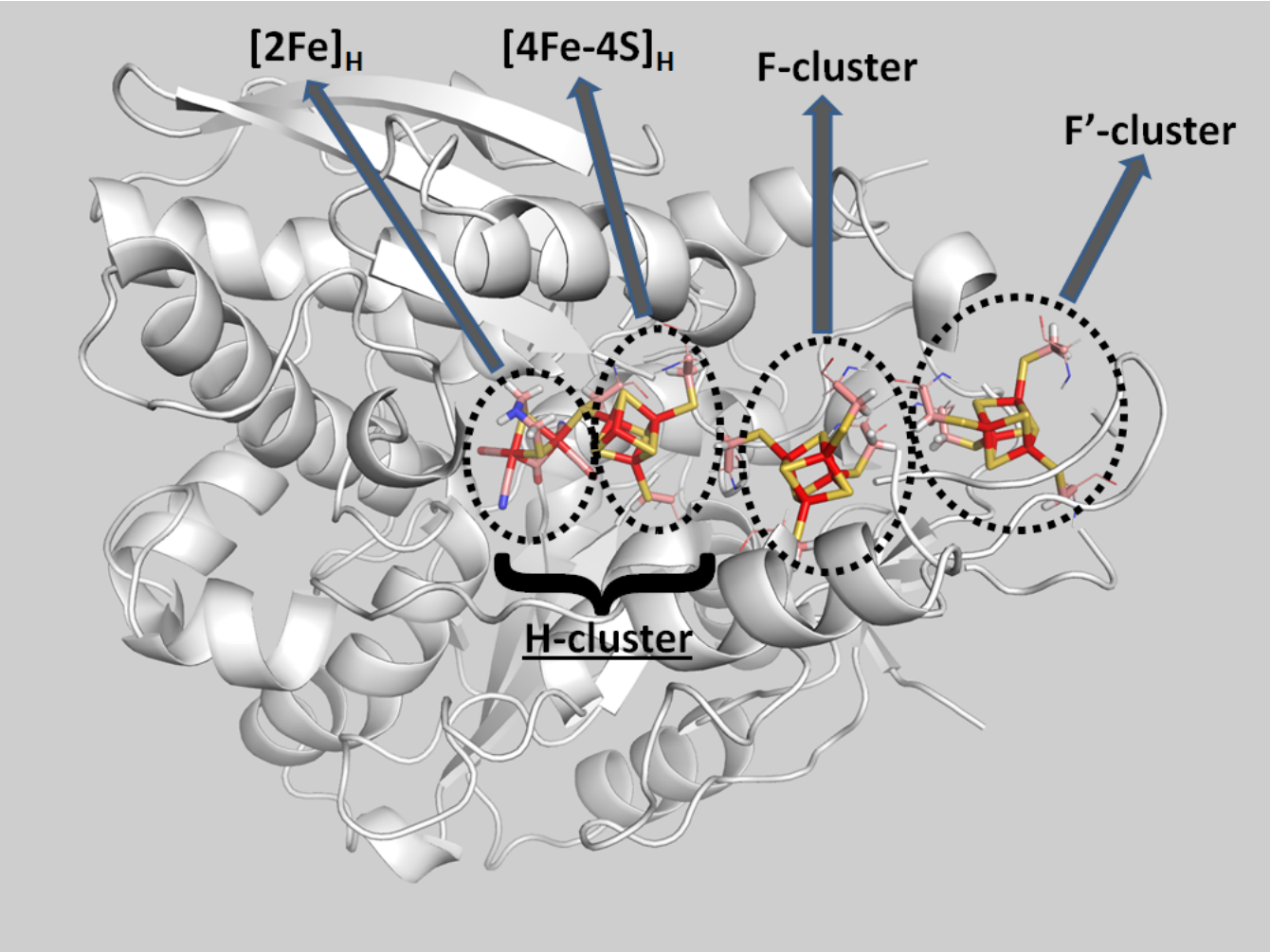

Figure 2. Arrangement of Fe–S clusters in the [FeFe]-hydrogenase from *D. desulfuricans* (DdH).

Differently from several [FeFe]-hydrogenases variants that are irreversibly inactivated when purified in aerobic and non-reducing conditions (e.g. the two [FeFe]-hydrogenases expressed by *Clostridium pasteurianum*, CpI and CpII), DdH and DvH can be activated after aerobic purification.[12a] The aerobically purified enzyme (DH_{oxair} in the following) is over-oxidized and inactive. EPR measurements have shown that DH_{oxair} is diamagnetic, which implies that all the Fe_4S_4 assemblies (i.e. the $[4Fe{-}4S]_H$, F, and F' moieties) are in the oxidized, 2Fe(II)2Fe(III) state.[17] However, reductive titration experiments at temperatures lower than 80 K showed that DH_{oxair} can be converted into an EPR-active form. In particular, the intensity of the EPR signal was reported to reach its maximum at –110 mV and starts declining at potentials more negative than –200 mV.[20] Concomitantly with the decrease of the first EPR

signal, another EPR signal appears, which was shown to dominate the EPR spectrum at potentials around –250 mV.[20] Both signals were ascribed to the catalytic H-cluster, more specifically to a transient enzyme state (DH_{trans}) in which the $[4Fe{-}4S]_H$ subcluster is reduced to the 3Fe(II)Fe(III) state, and to the active-ready form of the enzyme (DH_{ox}), in which the $[2Fe]_H$ subcluster has become paramagnetic as a result of a one-electron reduction at the expense of the $[4Fe{-}4S]_H$ subcluster.[21] Such an electron transfer within the H-cluster in the DH_{trans}/DH_{ox} transition was proposed to be triggered by an H-cluster conformational rearrangement, the details of which are presently unknown.[17,21] However, it has been also proposed that the DH_{trans}/DH_{ox} conversion implies two-electron reduction [W. Roseboom, A. L. De Lacey, V. M. Fernandez, E. C. Hatchikian, S. P. J. Albracht, J. Biol. Inorg. Chem. 2006, 11, 102-118].

In DH_{ox} the accessory F and F' clusters attain the diamagnetic 2Fe(II)2Fe(III) redox state. In fact, no signals assignable to the F and F' clusters could be detected in the enzyme EPR spectrum at potentials less negative than –250 mV.[20] The EPR signal of DH_{ox} reaches the maximum intensity at –300 mV, but at –320 mV it suddenly disappears, while the concomitant development of a complex EPR signal is observed, the latter featuring a midpoint potential of –305 mV. This complex EPR signal was attributed to the completely reduced enzyme (DH_{red}), featuring an EPR-silent H-cluster and EPR-active F and F' clusters in the reduced 3Fe(II)Fe(III) state.[16,20]

While states like DH_{oxair} and DH_{trans} are not observed in all known [FeFe]-hydrogenases because the reductive activation is relevant only for enzymes that can be purified aerobically, the partially oxidized DH_{ox} state has counterparts in all [FeFe]-hydrogenases that have been studied by EPR.[12a,17] In fact, the DH_{ox} state of the enzyme, together with the DH_{red} state, play a crucial role in catalysis.[17] However, while DH_{red} is thought to correspond to a mixture of different protonation states of the enzyme[22] and its detailed structural features are still matter of debate, a clear picture of the structural features of the H-cluster in the DH_{ox} state is presently available. In DH_{ox}, the iron atom of the $[2Fe]_H$ subcluster distal relative to the $[4Fe{-}4S]_H$ cluster (Fe_d, see Figure 1; the second iron atom in $[2Fe]_H$ is termed proximal, Fe_p) is characterized by a vacant coordination position in trans to the μ-CO ligand, where ligands such as H_2O or H_2 can be loosely bound.[5,11,16,17,23] Indeed, the catalytic cycle for H_2 oxidation is thought to

imply initial binding of the H_2 molecule to the Fe_d atom of the enzyme in the DH_{ox} state, followed by heterolytic cleavage of H_2 mediated by the DTMA amine group, and eventually proton and electron release from the enzyme.[9-11]

Prompted by the above observations, we have taken advantage of the wide knowledge on the DH_{ox} redox state to carry out a combined quantum mechanical and molecular mechanics (QM/MM) investigation of the DdH enzyme, in which the electronic properties of all Fe–S clusters in the protein (H-cluster + Fe_4S_4 clusters) have been explicitly described using DFT. The main goal of the study was the elucidation of the interplay among the Fe–S clusters in the DH_{ox} redox state of [FeFe]-hydrogenases, as well as the evaluation of the influence of substrate (H_2) and ligand (H_2O) binding on the electronic and functional properties of the enzyme.

Methods

QM/MM approaches based on DFT modeling of the QM region have already proved reliable for the characterization of the electronic properties of large subsystems within proteins.[24] However, the extensive inclusion of Fe–S clusters in the QM region represents a challenge, because these assemblies usually present antiferromagnetic coupling, as in the case of the $[4Fe{-}4S]_H$, F, and F' clusters. Such an issue can be tackled by using the broken-symmetry (BS) approach[25,26] and fast methods for the generation of BS states.[27]

All QM/MM calculations were based on the 1.6-Å resolution structure of DdH (PDB code 1HFE), a heterodimer composed of a small and a large subunit.[1] In the QM/MM calculations, the protein is divided into two subsystems: System 1 is treated at QM level and it is allowed to relax. It consists of the atoms in the H, F, and F' clusters (see below). The remaining portion of the protein, together with the surrounding water molecules, were included in system 2, which is kept fixed at the crystallographic coordinates and is treated at MM level. However, before starting the QM/MM optimization, it is necessary to add the hydrogen atoms that are not detected in the X-ray investigation of the protein. The

protonation state of histidine sidechains was assigned as previously reported.[11,23] All Lys and Arg residues were considered in their positively charged state, while Asp and Glu side chains were included in the anionic form. Finally, the iron-bound Cys residues (i.e. amino acids 36, 38, 41, 45, 66, 69, 72, 76, 179, 234, 378 and 382) were assumed to be deprotonated. As a result, the overall charge of the models (full protein, including the inorganic portion, plus solvent) is zero in the case of **DH_{ox}**, **DH_{ox}-H_2** and **DH_{ox}-H_2O**, whereas it is +2 for **DH_{ox+2}**, **DH_{ox+2}-H_2O**, and **DH_{ox_5CO}** (*vide infra* for details on the composition of the QM region of the models).

After addition of the hydrogen atoms to the crystal structure, the protein was solvated in a sphere of water molecules with a radius of 48 Å with the Amber leap module. In order to optimize the positions of hydrogen atoms and solvent water molecules, a 90 ps simulated-annealing molecular dynamics calculation was carried out, followed by 10000 steps of conjugate-gradient energy minimization, keeping all the other atoms fixed at their positions in the crystal structure. All the metal-bound ligands found in the PDB file were included in the QM/MM model, except a water molecule bridging Fe_d and Fe_p, which was replaced by a carbonyl group, following a more recent correction to the original crystal structure.[2]

All the QM/MM optimizations were carried out with the COMQUM program,[28,29] using TURBOMOLE[30] for the QM part and AMBER 8[31] (with the Amber 1999 force-field)[32] for the MM part. The QM calculations were carried out within the density functional theory (DFT) framework, using the B3LYP functional[33,34] and an all-electron SVP basis set with polarization functions on all atoms.[35] The use of the SVP basis has been previously validated.[27] B3LYP gives unpaired spins distributions that are in better agreement with EPR and Mössbauer experimental data when compared with results obtained using pure functionals.[36] However, calculations were carried out also at the BP86/SVP level, and the conclusions one can draw from the latter results are compatible with the picture coming from B3LYP/SVP optimizations (see Supporting Information).

The antiferromagnetic coupling that characterizes the Fe_4S_4 assemblies included in the QM region of the QM/MM model was treated by means of the BS approach.[25-27] Details on the BS scheme used are given in the Supporting Information section.

In the QM calculations, all atoms in system 2 are represented by a partial point charge. These charges are included in the Hamiltonian of the QM calculations, and thus the quantum-chemical system is polarized by the atoms of system 2 in a self-consistent way. When the quantum and classical regions are connected by a chemical bond, the hydrogen link-atom approach is applied,[37] i.e. the QM system is truncated with hydrogen atoms, the positions of which are linearly related to the corresponding carbon atom in the protein. The total QM/MM energy is calculated as:

$$E_{QM/MM} = E_{QM1} + E_{MM12} - E_{MM1} \quad (1)$$

Here, E_{QM1} is the QM energy of the quantum system truncated by hydrogen atoms, including the interaction between system 1 and the surrounding point charges. E_{MM1} is the MM energy of the quantum system, still truncated by hydrogen atoms, but without any electrostatic interactions. Finally, E_{MM12} is the classical energy (including non-bonded interactions between the QM and MM part) of all the atoms in the system with carbon atoms at the junctions and with the charges of the QM region zeroed, to avoid double counting of the electrostatic interactions. Such an approach, which is similar to the one used in the Oniom method [Svensson, M.; Humbel, S.; Froese, R. D. J.; Matsubara, T.; Sieber, S.; Morokuma, K. *J. Phys. Chem.* **1996**, *100*, 19357-19363.], should lead to the cancellation of errors caused by the truncation of the quantum system. [NOTE FOR ULF: we added this part because Referee 2 asked about the non-bonded interactions between the QM and the MM parts]

The QM system (system 1) of the various [FeFe]-hydrogenase models always included the iron and sulfide ions of the Fe_6S_6 H-cluster and of the Fe_4S_4, F and F' clusters, the DTMA ligand, three CO groups, two CN ligands (in the all-CO model, these two ligands were replaced by two CO ligands), and

twelve CH_3S fragments that represent the Cys residues connecting the H, F, and F' clusters to the rest of the enzyme large subunit. Some of the models included also an additional H_2 or H_2O ligand, as specified in the Results and Discussion section. The total number of atoms in the QM system thus varies between 106 and 109.

We have also carried out multiple 10 ns molecular dynamics simulations to test the structural stability of the models used in QM/MM calculations and to verify that the changes in the electronic structures of the Fe–S clusters do not affect significantly the conformation of the surrounding residues. Details about these calculations are reported in the Supporting Information.

Results and Discussion

Characterization of the electronic structure of the active-ready DH_{ox} enzyme state

A fundamental premise for the investigation of the effects of ligand binding on the electronic properties of the Fe–S clusters of [FeFe]-hydrogenases is the reliable assignment of the H-cluster redox state in the DH_{ox} state. As mentioned in the Introduction, the EPR data[20] available for the DH_{ox} enzyme form indicate that both the $[4Fe\text{-}4S]_H$ subcluster and the F and F' clusters are in the diamagnetic 2Fe(II)2Fe(III) state. As for the $[2Fe]_H$ subsite, comparisons between experimental and computed vibrational frequencies, as well as EPR parameters, indicate a Fe(I)Fe(II) state.[22,38] Such a picture is supported also by complementary data collected studying biomimetic organometallic compounds[39-41] and small-size QM models of either the whole H-cluster[42] or its binuclear subsite.[22,43] However, as recently noticed by Lubitz et al.,[17] Mössbauer data on DH_{ox} are also compatible with a $[2Fe]_H$ subsite attaining the Fe(II)Fe(III) redox state. Moreover, in a recent QM/MM study, it was suggested that a catalytic cycle involving Fe(II)Fe(III) species has a reasonable energy profile.[44] Therefore, we have initially used our QM/MM model of the *Desulfovibrio* enzyme to evaluate if the Fe(II)Fe(III) and Fe(II)Fe(I) redox states of the $[2Fe]_H$ subsite are compatible with the simultaneous presence in DH_{ox} of

diamagnetic $[4Fe\text{-}4S]_H$, F and F' clusters featuring the 2Fe(II)2Fe(III) redox state. In particular, we have first carried out QM/MM geometry optimization of an enzyme form (**DH_{ox+2}**) characterized by a –5 total charge of the QM subsystem (see Methods for details), which formally corresponds to a Fe(II)Fe(III) redox state of the $[2Fe]_H$ subcluster and a 2Fe(II)2Fe(III) redox state of the $[4Fe\text{-}4S]_H$, F, and F' clusters, respectively (here and in the following we formally assign the charge and spin of the bridging Cys ligand to the $[4Fe–4S]_H$ subcluster).

The QM/MM results clearly show that the Fe(II)Fe(III) state of the $[2Fe]_H$ subsite is not compatible with the presence of $[4Fe\text{-}4S]_H$, F, and F' clusters in the 2Fe(II)2Fe(III) redox state. In fact, in the optimized **DH_{ox+2}** model (Figure 3) the $[2Fe]_H$ subcluster features a total charge as low as –0.5, i.e. approximately 1.5 *e* more negative than the +1 formal charge corresponding to the Fe(II)Fe(III) state. In addition, the F-cluster reaches a charge and spin population of –1.2 and –0.8, respectively, indicating formation of an oxidized Fe(II)3Fe(III) state instead of the experimentally observed 2Fe(II)2Fe(III) state. Therefore, the analysis of the electronic structure of **DH_{ox+2}** indicates that the $[2Fe]_H$ subcluster posed at the Fe(II)Fe(III) redox state would spontaneously evolve towards a Fe(II)Fe(II) state, with concomitant oxidation of the F-cluster.

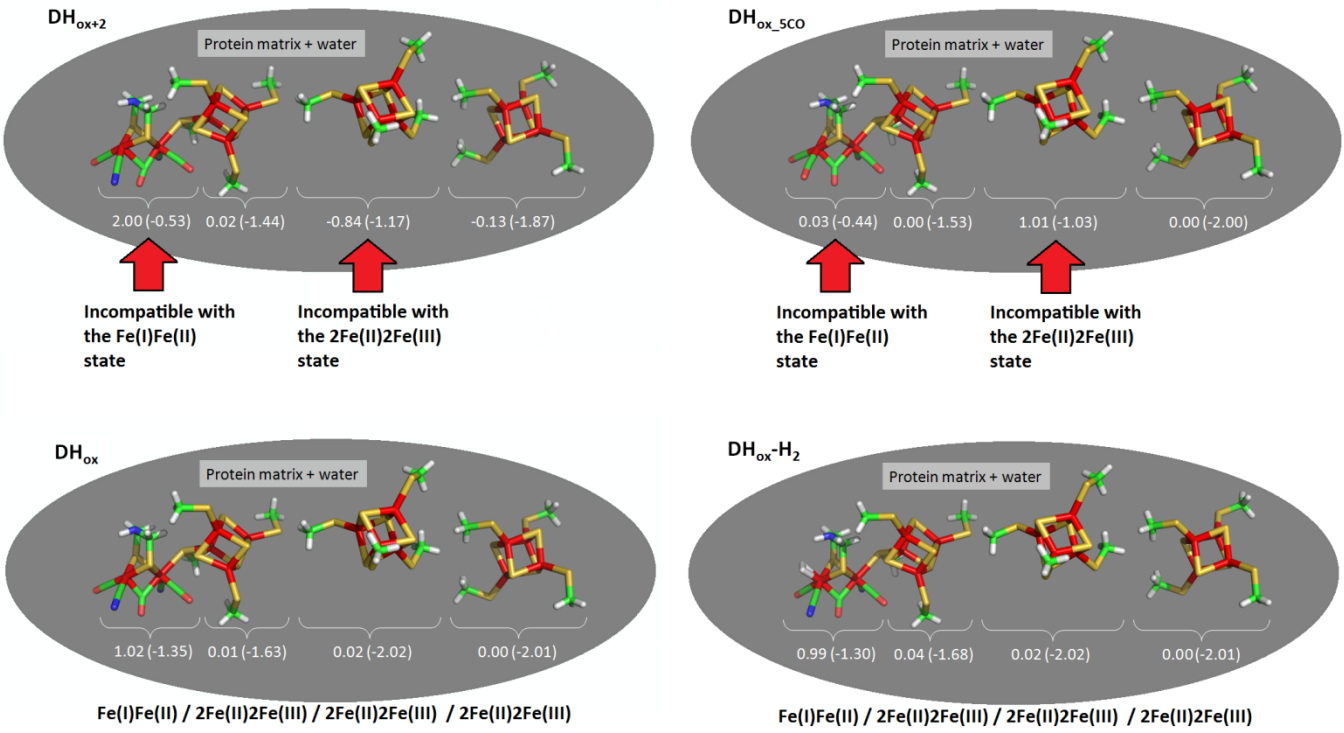

Figure 3. Geometries, spin populations, charges (in brackets) and formal oxidation states of the Fe–S clusters in the QM/MM models **DH_{ox+2}**, **DH_{ox}**, **DH_{ox}-H_2**' and **DH_{ox_5CO}**. The following atom colors are used: red for Fe, yellow for S, white for H, blue for N, green for C, and light red for O. The Fe_d–Fe_p and Fe_p–S(Cys) bond lengths, as well as the average bond lengths between the iron ions and the cysteine sulfur atoms in the $[4Fe–4S]_H$, F, and F'-clusters are: 2.68, 2.44, 2.31, 2.28, 2.30 Å in **DH_{ox+2}**, 2.55, 2.44, 2.31, 2.33, 2.31 Å in **DH_{ox}**, 2.65, 2.52, 2.31, 2.33, 2.31 Å in **DH_{ox}-H_2,** and 2.62, 2.44, 2.31, 2.26, 2.31 Å in **DH_{ox_5CO}**, respectively.

Addition of two electrons to the **DH_{ox+2}** model results in a species (**DH_{ox}**) that, after optimization, is characterized by zero spin population at the $[4Fe\text{-}4S]_H$, F, and F' clusters (Figure 3), as expected for diamagnetic Fe_4S_4 clusters, while the unpaired electron is localized on the $[2Fe]_H$ subcluster, in agreement with EPR and Mössbauer results for the DH_{ox} state.[20,21] Moreover, the F and F' clusters have Mulliken charges close to the formal –2 charge expected for a 2Fe(II)2Fe(III) state. In addition, the overall charge of the H-cluster (–3.0) is compatible with a Fe(I)Fe(II)–2Fe(II)2Fe(III) redox state. Therefore, we can confidently conclude that in the DH_{ox} state, the $[2Fe]_H$ subcluster is characterized by the Fe(I)Fe(II) redox state. Similar results are obtained by calculations carried out on **DH_{ox}** and **DH_{ox+2}** variants featuring a water molecule weakly bound to Fe_d (models **DH_{ox+2}-H_2O** and **DH_{ox}-H_2O**, see Supporting Information).

Role of CN ligands on the redox properties of DH_{ox}

A key issue in hydrogenases chemistry is the role played by the biologically unusual cyanide ligands. We have recently reported that the cyanide ligands are crucial for the proper redox interplay between the two subclusters that compose the H-cluster. In fact, we showed that the substitution of both CN ligands with carbonyls would impair the ability of the $[2Fe]_H$ cluster to reach the Fe(I)Fe(II) redox state upon one-electron oxidation of the reduced H-cluster, a fact that is expected to lower the electrophilicity of the enzyme active site and its affinity towards H_2.[45] These previous observations prompted us to study the role of cyanide ligands on the electronic properties of the whole chain of Fe–S clusters in DdH. To this end, we substituted the two CN ligands in the $\mathbf{DH_{ox}}$ model with CO groups, obtaining the model $\mathbf{DH_{ox\_5CO}}$ (see Fig. 3). After QM/MM geometry optimization, the electronic structure analysis showed that CN/CO substitution has a large impact not only on the H-cluster electronic structure, as previously noted, but also on the other Fe–S clusters. In fact, in $\mathbf{DH_{ox\_5CO}}$ the $[2Fe]_H$ subcluster switches from the paramagnetic Fe(I)Fe(II) state to a diamagnetic state, as deduced by comparison of the $[2Fe]_H$ spin populations in $\mathbf{DH_{ox}}$ and in $\mathbf{DH_{ox\_5CO}}$ (1.0 and 0.0, respectively; see Figure 3). Moreover, the overall charge of the H-cluster in $\mathbf{DH_{ox\_5CO}}$ (–2.0, Figure 3) is compatible with a formal Fe(I)Fe(I)–2Fe(II)2Fe(III) redox state. This means that the $[2Fe]_H$ subcluster reaches a lower oxidation state in $\mathbf{DH_{ox\_5CO}}$, when compared to the $\mathbf{DH_{ox}}$ model. Concomitantly, the F-cluster is oxidized and reaches the paramagnetic Fe(II)3Fe(III) state in $\mathbf{DH_{ox\_5CO}}$ (Mulliken charge and spin population = –1.0 and 1.0, respectively).

A comparison between energy diagrams of molecular orbitals in $\mathbf{DH_{ox}}$ and $\mathbf{DH_{ox\_5CO}}$ visualizes further key details of the effects of CN/CO substitutions on the electronic properties of the enzyme. In fact, Figure 4 shows that the highest occupied molecular orbitals (HOMOs) in $\mathbf{DH_{ox}}$ are localized on the H-cluster, while the occupied MOs centered on the F'-cluster are found at energy values that are at least 1.3 eV lower than the HOMO energy level. Conversely, in $\mathbf{DH_{ox\_5CO}}$ the HOMOs are localized not only on the H-cluster, but also on the F'-cluster, whereas the MOs localized on the F-cluster are shifted to

relatively lower energies. The latter is a result of the above-mentioned one-electron oxidation of the F-cluster upon CN/CO substitutions in the H-cluster. Finally, also the distribution of unoccupied MOs in the two energy diagrams of Figure 4 is significantly different. Most notably, the lowest unoccupied molecular orbital (LUMO) is localized on the F'-cluster in $\mathbf{DH_{ox}}$, whereas it is centered on the F-cluster in $\mathbf{DH_{ox\_5CO}}$.

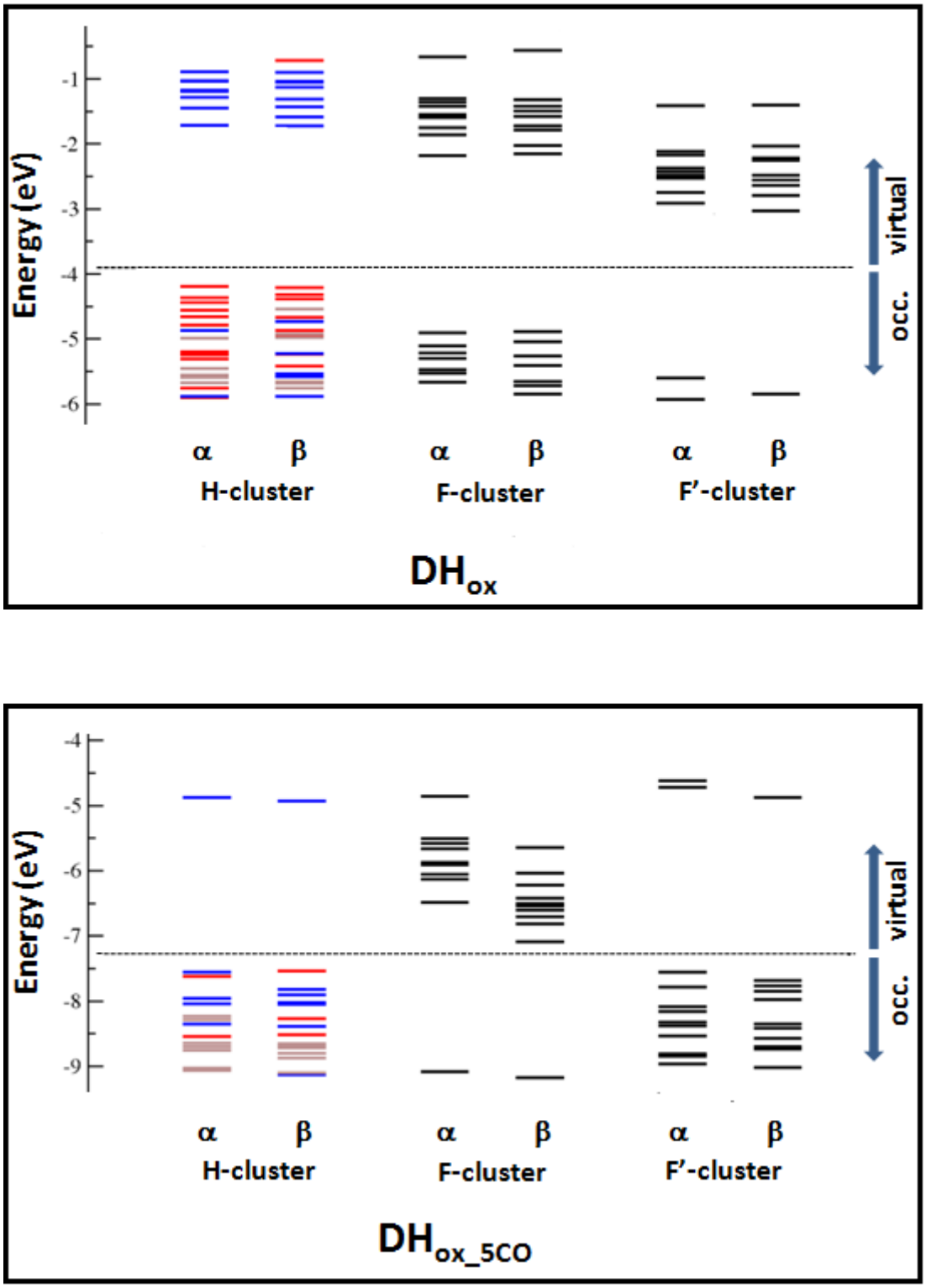

Figure 4. Detailed orbital diagrams of models **DH$_{ox}$** and **DH$_{ox_5CO}$**. The dotted horizontal line marks the separation between occupied and unoccupied orbitals. MOs localized on the H-cluster are distinguished by the use of different colors (red, blue or grey for orbitals centered on the $[2Fe]_H$ subcluster, on the $[4Fe\text{-}4S]_H$ subcluster, or delocalized over these two subclusters, respectively).

Effects of substrate (H_2) and ligand (H_2O) binding on the electronic properties of the DH_{ox} redox form of the enzyme

As mentioned above, the partially oxidized DH_{ox} form of the enzyme is involved in H_2 binding.[17,42,43] In particular, in [FeFe]-hydrogenases that are physiologically involved in H_2 uptake, binding of H_2 to the $[2Fe]_H$ subcluster was proposed to be immediately followed by H_2 oxidation and concomitant F-cluster reduction (e.g. in CpII). This picture, originally proposed by Adams,[12a] is supported by the experimental observation that the F-clusters in CpII feature redox potentials between –180 and –300 mV, much less negative than that of the H-cluster (–410 mV). On the contrary, in the CpI hydrogenase – which is "reversible", meaning that it is able to efficiently catalyze both the reduction of protons and H_2 oxidation – the redox potentials of the H-cluster and of the ancillary clusters are very close to each other,[12a] such that electrons can be easily mobilized both towards and from the active site. Adams proposed that in the case of H_2 binding to reversible hydrogenases, there is no immediate oxidation of H_2 with concomitant reduction of one of the F-clusters, because of the relatively low redox potential of the latter.[12a] In view of these observations, we have investigated the effects of H_2 binding to Fe_d on the electronic structure of the DdH, which is a reversible hydrogenase as well. To this end, a model in which a H_2 molecule is coordinated to the Fe_d atom of the DH_{ox} form (**DH_{ox}-H_2**) was optimized and analyzed.

Comparison of Mulliken charges and spin populations in **DH_{ox}-H_2** and **DH_{ox}** (Figure 3) suggests that the redox state of the Fe–S clusters is not affected by H_2 binding. However, fine modifications of the electronic structure of the enzyme upon H_2 binding are evident and can be highlighted comparing molecular orbitals of the **DH_{ox}-H_2** and **DH_{ox}** models (Figures 4 and 5).

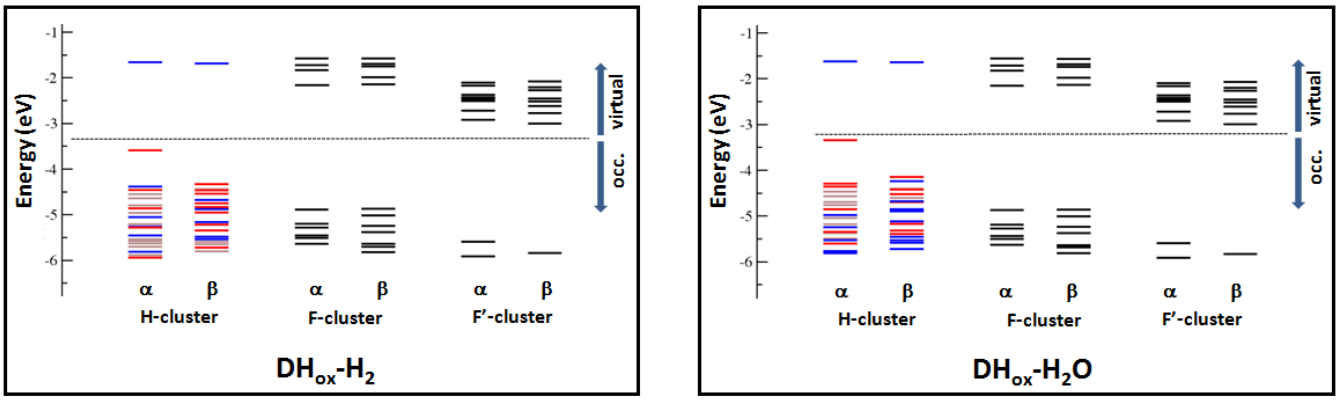

Figure 5. Detailed orbital diagram of models **DH_{ox}-H_2** and **DH_{ox}-H_2O**. The dotted horizontal line marks the separation between occupied and unoccupied orbitals. MOs localized on the H-cluster are distinguished by the use of different colors (red, blue or grey for orbitals centered on the $[2Fe]_H$ subcluster, on the $[4Fe\text{-}4S]_H$ subcluster, or delocalized over these two subclusters, respectively).

In the case of **DH_{ox}**, one can notice that the unoccupied MOs localized on the F'-cluster are among the lowest-lying virtual orbitals: They are found approx. 1.2 eV above the HOMO level, see Figure 4. Such a feature is functional for a facile reduction of the F'-cluster, which is the most solvent-exposed Fe–S site, thus prone to interactions with the physiological redox partners of the enzyme.

As far as H_2 binding is concerned, it is worth noting that **DH_{ox}** features a low-lying virtual orbital localized on the H-cluster binuclear subsite (Figure 4). As mentioned in a previous work,[42] an MO with these characteristics is ready to interact with the electron density of the H–H bond in H_2, thus explaining the electrophilic behavior of **DH_{ox}** and the ability of this enzyme state to bind H_2. Accordingly, it is not surprising to find that the HOMO of the H_2-bound adduct **DH_{ox}-H_2** is localized on the enzyme active site (see the MOs energy ranking of the latter model, reported in Figure 5).

As far as the LUMO in **DH_{ox}-H_2** is concerned, it is localized on the F'-cluster, not differently from the case of **DH_{ox}**. However, the HOMO–LUMO gap is significantly smaller in **DH_{ox}-H_2** than in **DH_{ox}**: 0.6 vs. 1.2 eV, respectively (see Figures 4 and 5). Such shrinking of the energy gap, which is induced by H_2

binding, suggests that the F'-cluster might withdraw one electron from the H-cluster when an exogenous polarizing species is bound to the enzyme.

In this context, it is worth underlining that in the H_2 oxidation reaction catalyzed by [FeFe]-hydrogenases, H_2 is not the only substrate of the enzyme, since during catalysis electrons are transferred from the enzyme to physiological redox partners,[12a] like cytochrome c_{553} [Verhagen MFJM, Wolbert RBG, Hagen WR, Eur. J. Biochem. 221, 821-829 (1994)]. Binding of such physiological redox partners is expected to affect the electronic structure of [FeFe]-hydrogenases, withdrawing electron density from the active site and possibly triggering $[2Fe]_H$ subcluster oxidation and H_2 activation. In fact, it was shown that heterolytic H_2 cleavage takes place only when the $[2Fe]_H$ subcluster is in the Fe(II)Fe(II) redox state (i.e. a state which is one electron more oxidized than in the resting DH_{ox} form).[11] Unfortunately, the computational study of intermolecular electron transfer is currently problematic because of the large size of the protein–protein complex, and also because no crystal structure of the DdH–cytochrome c_{553} complex is available [Morelli X, Czjzek M, Hatchikian CE, Bornet O, Fontecilla-Camps JC, Palma NP, Moura JJG, Guerlesquin F, J. Biol. Chem., 275, 23204-23210 (2000)]. However, to test the hypothesis that the redox potential of the $[2Fe]_H$ subcluster would change upon H_2 binding, we have carried out a new set of QM/MM calculations in which the polarization effects due to the binding of redox partners to [FeFe]-hydrogenases was *qualitatively* evaluated by the introduction of electron-withdrawing probes, such as cationic species, in the MM region of the QM/MM models.

In particular, single-point SCF calculations on $\mathbf{DH_{ox}}$ and $\mathbf{DH_{ox}}$-$\mathbf{H_2}$ models have been carried out after replacement of the solvent water molecule closest to the F'-cluster with a probe characterized by an increasing positive charge (0.9, 1.2, 1.5, 1.7, 2 a.u., respectively). The effect of the cationic probe on the overall charge of the $[2Fe]_H$ and F' clusters is shown in Figure 6. It turned out that the polarizing effect of the cationic probe promotes electron transfer from the $[2Fe]_H$ subcluster to the F' cluster, while the overall charge of the $[4Fe\text{-}4S]_H$ and F cluster remains essentially unaffected (Figure 6). More importantly, oxidation of the $[2Fe]_H$ subcluster and concomitant reduction of the F' cluster is more favored in $\mathbf{DH_{ox}}$-$\mathbf{H_2}$ than in $\mathbf{DH_{ox}}$.

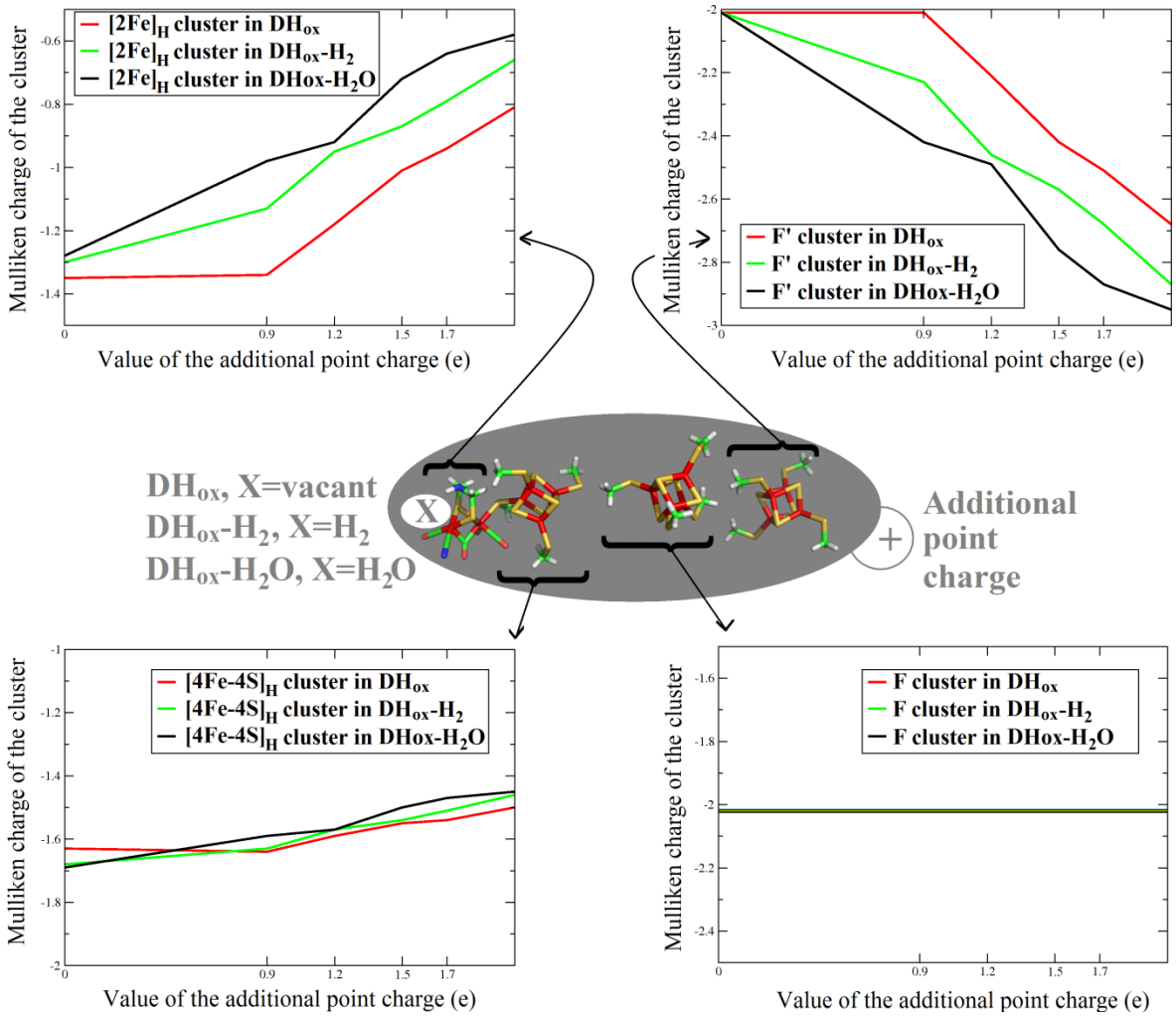

Figure 6. Variation of Mulliken charges of the $[2Fe]_H$, $[4Fe\text{-}4S]_H$, F, and F' clusters in models **DH_{ox}**, **DH_{ox}-H_2,** and **DH_{ox}-H_2O**, as a function of the increasing value of the additional point charge with which such models were supplemented.

This effect is functionally relevant, because it indicates that if a suitable polarizing or redox partner is bound in proximity of the F'-cluster, oxidation of the $[2Fe]_H$ cluster can be triggered by substrate binding.

As mentioned in the Introduction, a water molecule could be loosely bound to the distal iron atom in the DH_{ox} redox state of the enzyme. This observation prompted us to evaluate how the binding of a H_2O molecule to the H-cluster (**DH_{ox}-H_2O**) affects the electronic structure of the Fe–S clusters, using as reference the electronic structure of the **DH_{ox}-H_2** adduct. Notably, a schematic representation of

molecular orbitals reveals that the electronic structures of **DH_{ox}-H_2O** and **DH_{ox}-H_2** are extremely similar (Figure 5; see also the Supplementary Information for clusters charges and spin densities in **DH_{ox}-H_2O**). Therefore, according to our QM/MM calculations, binding of a water molecule could also facilitate electron transfer from the $[2Fe]_H$ subcluster to the F'-cluster, if a suitable polarizing molecule is bound close to the F'-cluster. However, binding of a H_2 molecule followed by one-electron oxidation of the Fe(I)Fe(II) $[2Fe]_H$ cluster increases the acidity of the metal-bound H_2 molecule to such an extent to trigger its heterolytic cleavage,[11] which eventually leads to release of two protons and two electrons from the enzyme, whereas H_2O binding leads to a dead-end reaction pathway that can be best described as a simple equilibrium between a Fe(II)Fe(I)-F'$_{ox}$ and a H_2O-Fe(II)Fe(II)-F'$_{red}$ species (Scheme 1). In this context, it is noteworthy that purified preparations of DdH at pH < 6 are inactivated in protein-film voltammetry experiments conducted at potentials higher than 0.05 V.[12b] Such inactivation was proposed to originate from a one-electron oxidation of DH_{ox},[12b] that would lead to a water-bound, inhibited $[2Fe]_H$ cluster attaining the Fe(II)Fe(II) state. The resulting H_2O-Fe(II)Fe(II) species is expected to easily reactivate upon one-electron reduction,[12b] thus defining an equilibrium analogous to the one above described for the enzyme-ferredoxin complex.

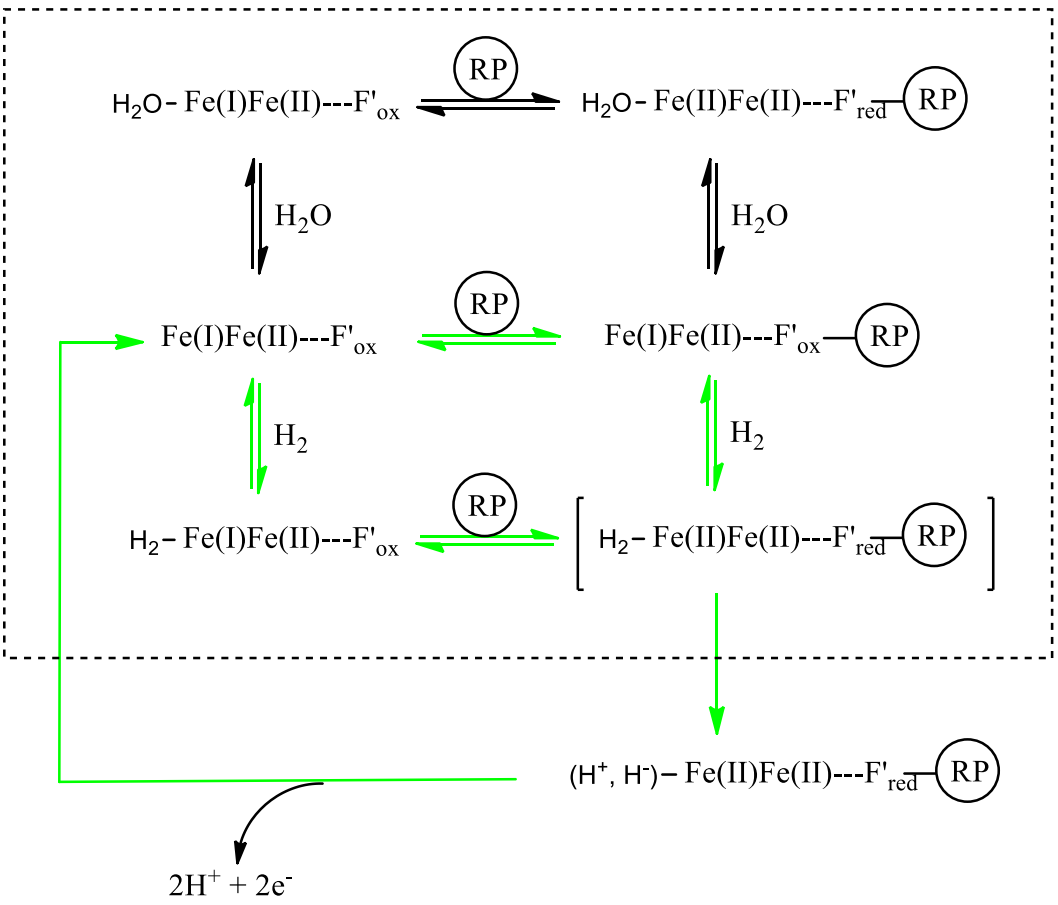

Scheme 1. Schematic representation of the reactivity of **DH$_{ox}$** with H_2, H_2O, and a generic redox partner (indicated as RP in the scheme). The oxidized 2Fe(II)2Fe(III) and reduced 3Fe(II)Fe(III) states of the F'-cluster are schematically indicated using the labels F'$_{ox}$ and F'$_{red}$, respectively. The enzyme forms discussed in this work are inside the dotted box. Reaction steps that are relevant in the catalytic cycle leading to H_2 oxidation are colored in green.

Conclusions

By using DFT in the context of a QM/MM, broken-symmetry representation of the [FeFe]-hydrogenase from *D. desulfuricans*, we have characterized fundamental properties of the enzymatic Fe–S cluster

chain. The approach applied here is based on the inclusion of the whole inorganic subsystem (H-cluster, F, and F' clusters) in the quantum-mechanical portion of the model. As a first step, we used such a model to show that the partially oxidized, active-ready form of DdH cannot attain the Fe(II)Fe(III) redox state at the catalytic $[2Fe]_H$ subsite. In fact, even though the Fe(II)Fe(III) state is compatible with previous Mössbauer results,[15,17] it turned out to be at odds with the actual relative redox potentials of the Fe–S assemblies in the enzyme. On the other hand, full consistency between theory and experiments is observed in the case of the alternative Fe(I)Fe(II) redox state.

Our QM/MM results confirm and extend previous findings, [Ref. OUR JACS INTERPLAY CN LIGANDS] indicating that the natural selection of biologically unusual CN ligands has a profound effect in terms of balancing the redox properties of the various clusters in the [FeFe]-hydrogenases. In fact, the replacement of the naturally occurring CN ligands with carbonyl groups would give place to a dramatic modification of DdH electronic structure.

We have also investigated the electronic effects of H_2 (substrate) binding to the H-cluster. It turned out that even though H_2 binding to the active-ready enzyme does not significantly influence the charges and spin populations of the clusters, it clearly leads to a decrease of the HOMO–LUMO gap. Such a reorganization of the electronic structure is relevant from a functional point of view, since the HOMO is localized on the H-cluster, while the LUMO is centered on the solvent-exposed F'-cluster. Therefore, a reduction of the gap between such molecular orbitals is expected to favor long-range electron transfer within the protein matrix. Actually, electron transfer from the H-cluster to the F'-cluster turned out to be favored in the H_2-bound form of DH_{ox}, when the polarizing effects of [FeFe]-hydrogenases redox partners (ferredoxins) are modeled by means of a simple point-charge representation. These results show the intimate connection between the electronic structure of the whole enzyme and its ability to establish a fruitful interplay with exogenous cellular redox partners of physiological importance. Such a biochemical issue has relevant bearings also on the quest for biomimetic reproduction of the enzyme function in organometallic compounds: In fact, in a recent contribution it was shown that proton-

coupled electron transfer involving mild oxidants can play a key role in the H_2 oxidation catalyzed by synthetic models of [FeFe]-hydrogenases.[46]

DdH is a "reversible" enzyme, meaning that it is able to efficiently catalyze the reaction $H_2 \leftrightarrows 2H^+ + 2e^-$ in both directions.[12,47] Our results support the hypothesis that this reversibility depends on the possibility to easily modulate the cluster redox potentials,[12a] to mobilize electrons along any of the two possible directions – i.e. towards the catalytically active H-cluster during H_2 evolution or towards the protein surface during H_2 oxidation – depending on the cellular metabolic state. Moreover, our findings let us envisage future perspectives for a targeted introduction of mutations in the enzyme, to change its specificity. In the case of DdH in particular, the introduction of positively charged residues (arginine or lysine moieties) spatially close to the F'-cluster might lead to polarization effects similar to those induced in our models by the charge probes used to simply mimicking the binding of a physiologically relevant redox partner. This might transform the reversible DdH enzyme into a monodirectional mutant featuring enhanced H_2-oxidizing properties.

Finally, we would like to remark that the theoretical approach presented here – i.e. studying a metalloenzyme by including its whole inorganic, redox-active portion in the high-level DFT treatment – may allow the characterization of some aspects of electron-transfer events of functional importance also in other classes of oxidoreductases featuring multiple Fe–S clusters.

Supporting Information Available. Discussion of the BS coupling scheme used for the models described in the paper; details on results obtained using an alternative BS coupling scheme as well as an alternative functional (BP86). **Xxx Also MD simulations.** This material is available free of charge via the internet at http://pubs.acs.org.

References.

(1) Nicolet, Y.; Piras, C.; Legrand, P.; Hatchikian, C. E.; Fontecilla-Camps, J. C. *Structure Fold. Design* **1999**, *7*, 13.

(2) Nicolet, Y.; de Lacey, A. L.; Vernede, X.; Fernandez, V. M.; Hatchikian, E. C.; Fontecilla-Camps, J. C. *J. Am. Chem. Soc.* **2001**, *123*, 1596.

(3) Peters, J. W.; Lanzilotta, W. N.; Lemon, B. J.; Seefeldt, L. C. *Science* **1998**, *282*, 1853.

(4) Pandey, A. S.; Harris, T. V.; Giles, L. J.; Peters, J. W.; Szilagyi, R. K. *J. Am. Chem. Soc.* **2008**, *130*, 4533.

(5) Lemon, B. J.; Peters, J. W. *Biochemistry* **1999**, *38*, 12969.

(6) Silakov, A.; Wenk, B.; Reijerse, E.; Lubitz, W. *Phys. Chem. Chem. Phys.* **2009**, *11*, 6592.

(7) Pilet, E.; Nicolet, Y.; Mathevon, C.; Douki, T.; Fontecilla-Camps, J. C.; Fontecave, M. *Febs Lett.* **2009**, *583*, 506.

(8) Ryde, U.; Greco, C.; De Gioia, L. *J. Am. Chem. Soc.* **2010**, *132*, 4512.

(9) Fan, H. J.; Hall, M. B. *J. Am. Chem. Soc.* **2001**, *123*, 3828.

(10) Siegbahn, P. E. M.; Tye, J. W.; Hall, M. B. *Chem. Rev.* **2007**, *107*, 4414.

(11) Greco, C.; Bruschi, M.; De Gioia, L.; Ryde, U. *Inorg. Chem.* **2007**, *46*, 5911.

(12) a) Adams, M. W. W. *Biochim. Biophys. Acta* **1990**, *1020*, 115. b) Parkin, A.; Cavazza, C.; Fontecilla-Camps, J. C.; Armstrong, F. A. *J. Am. Chem. Soc.* **2006**, *128*, 16808.

(13) Hatchikian, E. C.; Forget, N.; Fernandez, V. M.; Williams, R.; Cammack, R. *Eur. J. Biochem.* **1992**, *209*, 357.

(14) Pierik, A. J.; Hagen, W. R.; Redeker, J. S.; Wolbert, R. B. G.; Boersma, M.; Verhagen, M.; Grande, H. J.; Veeger, C.; Mutsaers, P. H. A.; Sands, R. H.; Dunham, W. R. *Eur. J. Biochem.* **1992**, *209*, 63.

(15) Popescu, C. V.; Munck, E. *J. Am. Chem. Soc.* **1999**, *121*, 7877.

(16) Albracht, S. P. J.; Roseboom, W.; Hatchikian, E. C. *J. Biol. Inorg. Chem.* **2006**, *11*, 88.

(17) Lubitz, W.; Reijerse, E.; van Gastel, M. *Chem. Rev.* **2007**, *107*, 4331.

(18) Voordouw, G.; Brenner, S. *Eur. J. Biochem.* **1985**, *148*, 515.

(19) Hatchikian, E. C.; Magro, V.; Forget, N.; Nicolet, Y.; Fontecilla-Camps, J. C. *J. Bacteriol.* **1999**, *181*, 2947.

(20) Patil, D. S.; Moura, J. J. G.; He, S. H.; Teixeira, M.; Prickril, B. C.; Dervartanian, D. V.; Peck, H. D.; Legall, J.; Huynh, B. H. *J. Biol. Chem.* **1988**, *263*, 18732.

(21) Pereira, A. S.; Tavares, P.; Moura, I.; Moura, J. J. G.; Huynh, B. H. *J. Am. Chem. Soc.* **2001**, *123*, 2771.

(22) Tye, J. W.; Darensbourg, M. Y.; Hall, M. B. *Inorg. Chem.* **2008**, *47*, 2380. Yu, L.; Greco, C.; Bruschi, M.; Ryde, U.; De Gioia, L.; Reiher, M. *Inorg Chem.* **2011**, 50, 3888.

(23) Greco, C.; Bruschi, M.; Heimdal, J.; Fantucci, P.; De Gioia, L.; Ryde, U. *Inorg. Chem.* **2007**, *46*, 7256.

(24) Guallar, V.; Wallrapp, F. *J. R. Soc. Interface* **2008**, *5*, S233.

(25) Noodleman, L.; Norman, J. G. *J. Chem. Phys.* **1979**, *70*, 4903.

(26) Noodleman, L. *J. Chem. Phys.* **1981**, *74*, 5737.
(27) Greco, C.; Fantucci, P.; Ryde U., De Gioia L, *Int. J. Quantum Chem.* **2010**, in press. DOI: 10.1002/qua.22849
(28) Ryde, U. *J. Comput.-Aided Mol. Des.* **1996**, *10*, 153.
(29) Ryde, U.; Olsson, M. H. M. *Int. J. Quantum Chem.* **2001**, *81*, 335.
(30) Ahlrichs, R.; Bar, M.; Haser, M.; Horn, H.; Kolmel, C. *Chem. Phys. Lett.* **1989**, *162*, 165.
(31) Case, D.A. et al. *Amber 8*; University of California: San Francisco, CA, 2004.
(32) Cornell, W. D.; Cieplak, P.; Bayly, C. I.; Gould, I. R.; Merz, K. M.; Ferguson, D. M.; Spellmeyer, D. C.; Fox, T.; Caldwell, J. W.; Kollman, P. A. *J. Am. Chem. Soc.* **1995**, *117*, 5179.
(33) Becke, A. D. *J. Chem. Phys.* **1993**, *98*, 5648.
(34) Lee, C. T.; Yang, W. T.; Parr, R. G. *Phys. Rev. B* **1988**, *37*, 785.
(35) Schafer, A.; Horn, H.; Ahlrichs, R. *J. Chem. Phys.* **1992**, *97*, 2571.
(36) Matito, E.; Sola, M. *Coord. Chem. Rev.* **2009**, *253*, 647.
(37) Reuter, N.; Dejaegere, A.; Maigret, B.; Karplus, M. *J. Phys. Chem. A* **2000**, *104*, 1720.
(38) Fiedler, A. T.; Brunold, T. C. *Inorg. Chem.* **2005**, *44*, 9322.
(39) Lyon, E. J.; Georgakaki, I. P.; Reibenspies, J. H.; Darensbourg, M. Y. *Angew. Chem.-Int. Ed.* **1999**, *38*, 3178.
(40) Le Cloirec, A.; Best, S. P.; Borg, S.; Davies, S. C.; Evans, D. J.; Hughes, D. L.; Pickett, C. J. *Chem. Commun.* **1999**, 2285.
(41) Schmidt, M.; Contakes, S. M.; Rauchfuss, T. B. *J. Am. Chem. Soc.* **1999**, *121*, 9736.
(42) Bruschi, M.; Greco, C.; Fantucci, P.; De Gioia, L. *Inorg. Chem.* **2008**, *47*, 6056.
(43) Cao, Z. X.; Hall, M. B. *J. Am. Chem. Soc.* **2001**, *123*, 3734.
(44) Trohalaki, S.; Pachter, R. *Int. J. Hydrogen Energ.* **2010**, *35*, 5318.
(45) Bruschi, M.; Greco, C.; Bertini, L.; Fantucci, P.; Ryde, U.; De Gioia, L. *J. Am. Chem. Soc.* **2010**, *132*, 4992.
(46) Camara, J. M.; Rauchfuss T. B. *J. Am. Chem. Soc.* **2011**, 133, 8098.
(47) Frey, M. *Chembiochem* **2002**, *3*, 153.

Synopsis TOC